



 Cite this: *RSC Adv.*, 2022, 12, 28997

# Highly efficient solar-absorber composite material based on tetrapyridylporphyrin for water evaporation and thermoelectric power generation†

 Yifeng Zhang,\* Hanbing Yan, Xuefeng Wang, Zhenyu Zhang,  Fengchun Liu, Shan Tu and Xiufang Chen

Photothermal materials based on organic small molecules have the characteristics of structural diversity and easy modification for solar-driven water evaporation and power generation technology. However, there still exist limitations, such as the utilization of solar energy and photostability. Therefore, it is the focus of current research to design organic photothermal materials with excellent photothermal stability, strong solar absorption capacity, and high photothermal conversion efficiency. Herein, photothermal conversion materials based on tetrapyridylporphyrin (TPyP) is studied, which possesses polypyrrole macrocyclic framework ( $18\pi$  electrons), which makes it exhibit strong absorption in the 300–800 nm region with high photothermal conversion. The interfacial-heating evaporation system based on polyurethane (PU) foam loaded with TPyP was prepared, whose solar-to-vapor conversion efficiency and vapor evaporation rate of PU + TPyP foam solar energy reached 56% and  $0.81 \text{ kg m}^{-2} \text{ h}^{-1}$ , respectively. In addition, TPyP-loaded solar evaporator equipped with abundant microchannels for water flow are integrated with thermoelectric devices, thus achieving an evaporation rate and voltage as high as  $0.69 \text{ kg m}^{-2} \text{ h}^{-1}$  and 60 mV under  $1 \text{ kW m}^{-2}$  solar irradiation, respectively. The successful application of TPyP in water evaporation and power generation effectively addresses the difficulties faced in the process of using organic small molecule photothermal materials to solve the energy crisis.

 Received 7th June 2022  
 Accepted 15th September 2022

DOI: 10.1039/d2ra03512j

[rsc.li/rsc-advances](http://rsc.li/rsc-advances)

## 1 Introduction

With the increasing world population, the shortage of fresh water resources in the world has been increasingly concerning. Fresh water resources are one of the indispensable materials for human survival. At present, the total amount of fresh water resources on Earth is very small, only 2.5% of the global water resources. Most of this water is found in the polar regions, where human density is low, and only 0.3% of all freshwater is actually available.<sup>1,2</sup> The global water output obtained by seawater desalination technology has also been significantly increased; thus, seawater desalination technology plays an important role in the sustainable development of human society for freshwater resource access.<sup>3</sup> Energy crisis is also another worldwide problem. Solar energy as clean energy has many advantages: it is non-polluting, there are abundant reserves with no geographical restrictions, and it does not need transportation to the point of use. The development of simple,

efficient, and flexible ways of using solar energy would provide an effective solution to seawater desalination and energy crisis. The conversion of solar energy to thermal energy, which is an efficient strategy for the direct acquisition of solar energy, can achieve high conversion efficiency and has a wide range of applications. When using photothermal materials to generate steam under sunlight irradiation, the heating mode has a significant effect on the solar-to-vapor efficiency and water evaporation rate. There are three ways to achieve solar evaporation: bottom heating evaporation, bulk evaporation, and interfacial evaporation.<sup>4,5</sup> At present, the most popular method is interfacial evaporation, which is inspired by plant transpiration. This method requires a photothermal material, a thermal insulator that isolates the photothermal material from bulk water, and a water transport channel through which liquid water can be transported to the evaporation interface. Compared with bulk evaporation, interfacial evaporation greatly reduces contact with bulk water and therefore heat loss. Since evaporation of water only occurs at the surface, heat must be concentrated on the air–water interface by photothermal materials to efficiently generate water vapor.<sup>6</sup> Thermoelectric power generation also provides a new strategy for providing an abundant supply of clean energy. This can be achieved by coating a photothermal material onto a blank thermoelectric sheet, the bottom of which is close to a circulating water tank.<sup>7</sup>

State Grid Shanxi Electric Power Research Institute, Taiyuan, Shanxi Province, 030012, P. R. China. E-mail: [zyf\\_dky@126.com](mailto:zyf_dky@126.com)

† Electronic supplementary information (ESI) available: The cooling curve of TPyP film after irradiation with 655 nm laser; the corresponding time–ln  $\theta$  linear curve of TPyP film; thermal conductivities of PU and PU + TPyP foams. See <https://doi.org/10.1039/d2ra03512j>



When the photothermal material on the upper side is irradiated with sunlight, heat is generated and this thermal energy can be converted into electrical energy. Therefore, it is urgent to develop photothermal materials with high efficiency of solar energy utilization.

Common photothermal materials mainly include carbon-based materials, metal-based nanoparticles, inorganic semiconductor materials, and organic polymers,<sup>8–20</sup> which are summarized in Table S1 of the ESI.† Although the water evaporation rate can reach a relatively high level, it is worth noting that photothermal materials such as precious metals and inorganic carbon-based materials are difficult to process and are costly, which limits their practical application.<sup>21</sup> Organic small-molecule materials have attracted growing attention due to their unique advantages in processing feasibility, structural diversity, and fine-tuned properties. At present, although biomedical applications have been thoroughly studied,<sup>22–28</sup> there are few studies on the use of organic small-molecule-based photothermal materials for solar energy conversion due to limited absorption spectra and low photothermal conversion efficiency.<sup>29–35</sup> Therefore, the development of organic small-molecule-based photothermal materials with excellent light absorption characteristics with wide light absorption range, high molar extinction coefficient, and excellent photothermal conversion efficiency is the key to achieve effective solar energy conversion.

Polycyclic  $\pi$ -conjugated materials have attracted much attention because of their unique molecular structure, excellent photoelectrical property, and thermostability. The aromatic compounds with large  $\pi$  conjugation degree generally possess relatively small energy level gap, resulting in an absorption spectrum redshift. The polycyclic  $\pi$ -conjugated materials possess strong intermolecular interaction, which could cause fluorescence quenching, thus improving nonradiative transition probability to convert heat in the aggregate state. Therefore, this category of molecules has the potential to be excellent solar-heat conversion materials.

Inspired by the structure of chlorophyll, which can convert solar energy to chemical energy efficiently when participating in photosynthesis, the key substances are porphyrin derivatives. Porphyrin derivatives are classic polycyclic conjugated compounds with polypyrrole macrocyclic framework (18 $\pi$  electrons), which possess intense molar extinction coefficient, relatively low fluorescence quantum yield, well photostability, and thermal stability. Herein, the porphyrin derivative tetrapyrrolylporphyrin (TPyP) is utilized as the photothermal material, which has a wide absorption region of 300–800 nm and high photothermal conversion efficiency 73.6% under 655 nm laser irradiation, and TPyP can be loaded onto polymers to form the functional composites through the interaction between the pyridine group and the polymeric carrier. Polyurethane (PU) foam was utilized as the substrate not only because its preparation process is simple and it has lower density than water, but also because it is porous and possesses low thermal conductivity.<sup>31</sup> The solar absorber composite PU + TPyP was prepared. Then, TPyP was loaded in the porous insulating PU foam to establish an effective solar evaporation system. The interfacial-

heating water evaporation system consisting of TPyP and PU foam possesses outstanding characteristics: efficient solar absorption, high photothermal conversion efficiency, excellent heat insulation, and superior porosity performance. The evaporation rate under 1 sun was up to 0.81 kg m<sup>-2</sup> h<sup>-1</sup>, and the solar-to-vapor conversion efficiency was 56%. To maximize the utilization of heat energy, a multifunctional device capable of simultaneous water evaporation and thermoelectric power generation was constructed by attaching a TPyP-loaded cellulose paper on a thermoelectric Peltier plate. With the presence of interface water evaporation within the TPyP-loaded cellulose paper, this proposed device realized a water evaporation rate of 0.69 kg m<sup>-2</sup> h<sup>-1</sup> and produced a stable voltage up to 60 mV as well under 1 kW m<sup>-2</sup> solar irradiation. Under hard sunlight, the microfan can be driven to rotate rapidly. This system successfully realizes the application of organic small-molecule photothermal materials in the area of water evaporation and thermoelectric power generation.

## 2 Results and discussion

### 2.1. Solar evaporator design, photophysical properties, and photothermal performance

Natural chlorophyll can efficiently absorb sunlight for photosynthesis and convert solar energy into chemical energy. The chlorophyll molecule contains a porphyrin ring and a long aliphatic hydrocarbon side chain. The role of the porphyrin (Py) ring in this molecule is to expand the intermolecular conjugation to broaden light absorption, and the aliphatic hydrocarbon side chain can improve the lipid solubility of the molecule. Py plays an important role in the field of photothermal applications due to its strong absorption spectrum of 300–400 nm (B-band) and 650–700 nm (Q-band), high molar absorption coefficient, and relatively low fluorescence quantum yield.<sup>36</sup> The main decay mode is non-radiative transition from the excited state back to the ground state of Pys after absorbing light energy, based on which Py can be potentially used as a photothermal material for solar-driven water evaporation and thermoelectric power generation. Therefore, tetrapyrrolyl porphyrins (TPyP) was used as the photothermal material, which possesses intense absorption spectrum of 300–800 nm in the solid state, as shown in Fig. 1a and b. Also, it shows a low fluorescence quantum yield ( $\phi_f$ ), which is evaluated to be only 2.03% in CHCl<sub>3</sub> solution (Fig. 1c).

The fluorescent emission property of TPyP can be severely quenched in the solid state, and the  $\phi_f$  is negligible, only 0.02%. It is worth noting that TPyP has a wide absorption spectrum, high molar extinction coefficient, lower solution, and solid  $\phi_f$ , which indicates that TPyP is a promising solar absorber material for water evaporation and thermoelectric power generation. As shown in Fig. S1, ESI,† there is no change in the quality under nitrogen atmosphere before 482 °C, which proves that no decomposition occurs before 482 °C, and TPyP has great thermal stability. The photothermal performance of TPyP was evaluated by an IR thermal camera, which quickly recorded the temperature change. As shown in Fig. 1d, 4 mg TPyP powder was irradiated under 730 nm laser (0.8 W cm<sup>-2</sup>). The



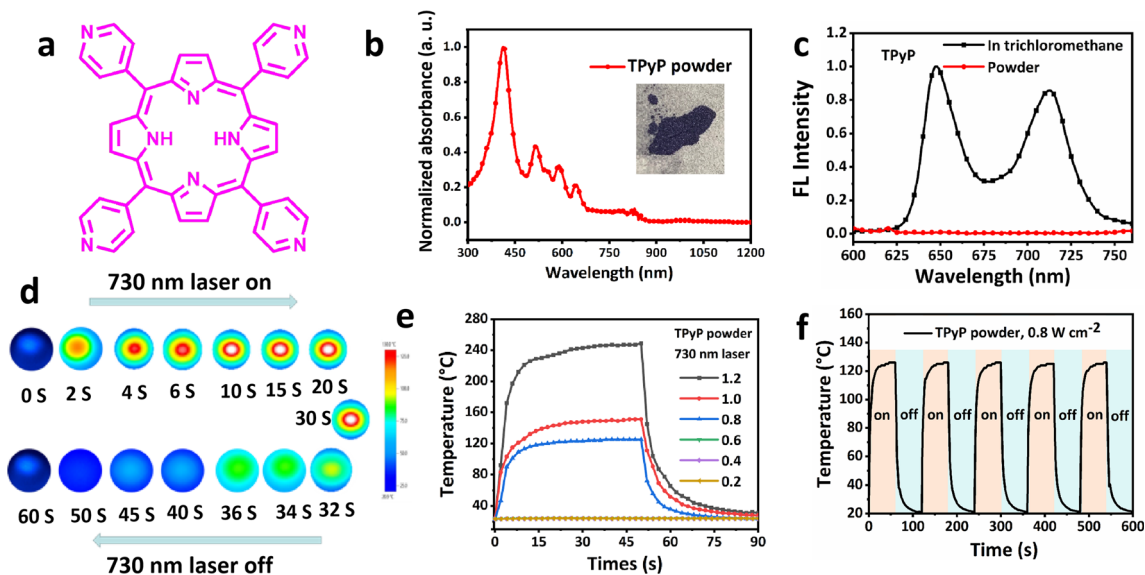


**Fig. 1** (a) The chemical structure of TPyP; (b) the absorption spectrum of TPyP powder. Inset shows the digital photo of TPyP powder taken under sunlight; (c) the photoluminescent (PL) spectra of TPyP in  $\text{CHCl}_3$  solution and powder. The excitation wavelength ( $\lambda_{\text{ex}}$ ) is 400 nm; (d) IR thermal images of TPyP powder (4 mg) under 730 nm laser irradiation ( $0.8 \text{ W cm}^{-2}$ ) and then turned off; (e) photothermal conversion behavior of TPyP powder under 730 nm laser irradiation at different laser power density ( $0.2, 0.4, 0.6, 0.8, 1.0,$  and  $1.2 \text{ W cm}^{-2}$ ); (f) anti-photobleaching property of TPyP powder (4 mg) during 5 cycles of heating-cooling processes.

temperature swelled sharply to about  $128 \text{ }^\circ\text{C}$  within 30 s, and then quickly shrank to room temperature after removing the laser, which showed excellent photothermal property, as shown in Fig. 1e. Under higher power density laser irradiation, the temperature rose up and the maximum temperature reached  $249 \text{ }^\circ\text{C}$  in 30 s under the 730 nm laser with a power density of  $1.2 \text{ W cm}^{-2}$ , which is positively correlated with the radiated power density of the 730 nm laser. The TPyP solid photothermal conversion efficiency was estimated to be 73.6% (Fig. S2 and S3, ESI†). Then, the TPyP powder was irradiated with 730 nm laser and turned the laser on and off for 5 cycles (Fig. 1f), and there was no temperature reduction in the photothermal conversion behavior.

## 2.2. PU + TPyP for water evaporation performance

TPyP is an organic photothermal material with excellent photothermal conversion property, which shows a wide absorption spectrum of 300–800 nm in the solid state and can effectively absorb and convert sunlight. To improve the efficiency of solar-driven water evaporation, an interfacial-heating seawater evaporation system was established. Compared with traditional solar evaporation technology, the interfacial evaporation system has great potential for practical application owing to its advantages of less heat loss and higher evaporation efficiency. PU foam was utilized as the substrate not only because its preparation process is simple but also it is porous and possesses low thermal conductivity.<sup>31</sup> Then, TPyP was loaded inside PU (cylinder, diameter: 2 cm, height: 1 cm) foam by impregnating PU foam in TPyP  $\text{CHCl}_3$  solution (5 mg dissolved in 1 mL  $\text{CHCl}_3$ ) and dried under  $50 \text{ }^\circ\text{C}$ , obtaining a brown color PU foam. The internal surface structure of PU foam with/

without TPyP could be characterized by scanning electron microscopy (SEM). The SEM images show that the surfaces of PU + TPyP are rougher than that of pure PU, which might promote surficial light management and facilitate photothermal conversion (Fig. 2a). Meanwhile, the thermal conductivity of the foam loaded without/with TPyP was 0.045 and  $0.045 \text{ W m}^{-1} \text{ K}^{-1}$  (Fig. S4, ESI†), respectively, proving that the PU + TPyP foam also has extremely low thermal conductivity, which could preserve maximum heat for water evaporation. Therefore, it is crucial to combine water transportation channel of foam and local heat of PU + TPyP, which can promote the water evaporation efficiency dramatically.

The temperature change of the PU + TPyP foam under 1 sun irradiation through a thermal infrared camera was monitored, as shown in Fig. 2b and c; the PU + TPyP foam loaded with 5 mg TPyP rose up to roughly  $50 \text{ }^\circ\text{C}$  within 50 s under 1 sun and reached an equilibrium temperature of  $52 \text{ }^\circ\text{C}$  after 10 min, while pure PU foam can only reach an equilibrium temperature of  $30 \text{ }^\circ\text{C}$  after 10 min. PU + TPyP foam can be used as the solar absorber of the interfacial-heating evaporation system because of its efficient sunlight absorption capacity, high photothermal conversion efficiency, well water transportation, and thermal-stability property. The system structure scheme is shown in Fig. 2d. Under 1 sun, obvious water vapor was visibly observed on the PU + TPyP foam surface. Then, the infrared thermal imaging camera continued to monitor the energy conversion efficiency from solar energy to water vapor, as shown in Fig. 2e. The temperature of the blank PU foam is much lower than the temperature of the PU + TPyP foam floating on the water at the same time. Under 1 sun, the equilibrium temperature of PU + TPyP foam can reach  $30.4 \text{ }^\circ\text{C}$  after 1 h, which is  $6 \text{ }^\circ\text{C}$  higher than that of the blank PU foam, proving that the introduction of PU +



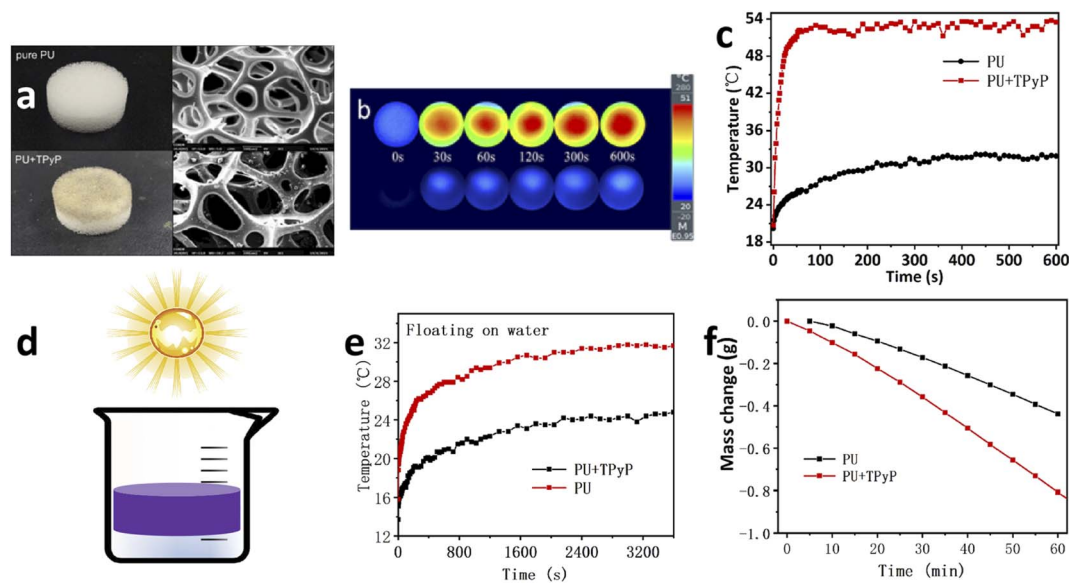


Fig. 2 (a) Digital photos and SEM images of PU and TPyP-loading PU (PU + TPyP) foams; (b) IR thermal images of PU + TPyP foams under 1 sun irradiation (top row); (c) photothermal conversion behavior of PU and PU + TPyP foams under 1 sunlight irradiation; (d) the schematic illustration of solar-driven water evaporation; (e) the temperature changes of PU and PU + TPyP foams floating on water under 1 sun irradiation; (f) water evaporation curves without (water only) and with PU foam or PU + TPyP foam under simulated sunlight with an intensity of  $1 \text{ kW m}^{-2}$ . The amount of TPyP used in preparing PU + TPyP foam is 5 mg.

TPyP foam promoted water evaporation effectively. Moreover, even after being irradiated for 4 h floating on the water, the temperature is almost not affected, as shown in Fig. S5 (ESI<sup>†</sup>), which reveals the excellent photostability of the TPyP foam.

In order to evaluate the water evaporation efficiency under sunlight irradiation, the device was used to measure the mass loss curve under 1 sun over time, and the mass was carefully recorded every 5 min. As shown in Fig. 2f, the evaporation rate of the PU + TPyP foam was dramatically increased to  $0.81 \text{ kg m}^{-2} \text{ h}^{-1}$ . The evaporation rate of the control group with PU was only  $0.44 \text{ kg m}^{-2} \text{ h}^{-1}$ . The experimental results confirmed that TPyP played a decisive role in the evaporation system based on PU + TPyP foam, which improved the evaporation efficiency. Moreover, the solar-driven conversion efficiency ( $\eta$ ) of PU + TPyP foam was calculated during the water evaporation process. The  $\eta$  of PU + TPyP foam with 5 mg TPyP was calculated to be 56%; the details are shown in the ESI<sup>†</sup>.

### 2.3. TPyP for thermoelectric power generation performance

The heat generated by TPyP under sunlight can also be used for thermoelectric power generation. As shown in Fig. 3a, 20 mg TPyP was coated on the blank thermoelectric generator (TEC1-12706, 40 mm 40 mm 3.6 mm), the back surface was tightly attached to the circulating water tank, forming a solar-drive thermoelectric power generation device. All thermoelectric data in this thermoelectric experiment are tested and obtained by the Keithley 6514 system. The temperature difference of the thermoelectric plate with TPyP increases, and the output voltage also increases under sunlight shown in Fig. 3b and c. The maximum temperature differences under 1, 2, and  $5 \text{ kW m}^{-2}$  sunlight irradiation were  $4.3 \text{ }^\circ\text{C}$ ,  $8.2 \text{ }^\circ\text{C}$ , and  $12.2 \text{ }^\circ\text{C}$ ,

respectively, and the corresponding maximum open-circuit voltages ( $V_{oc}$ ) was 104 mV, 208 mV, and 307 mV, respectively. In contrast, the maximum temperature difference of the blank thermoelectric sheet without TPyP coating is only  $2.5 \text{ }^\circ\text{C}$ , and the maximum  $V_{oc}$  is 41 mV. For the temperature difference of the power generation sheet under different light intensities, it can be clearly seen that the temperature difference of the device coated with photothermal material increases with the

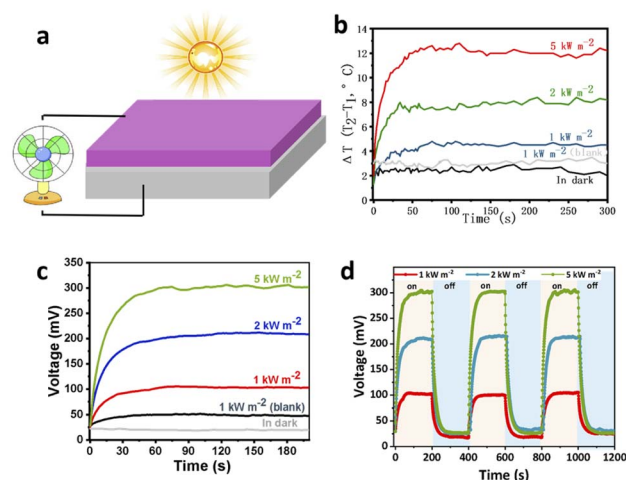


Fig. 3 (a) Schematic diagram of the thermoelectric device (purple layer: TPyP photothermal material, gray layer: thermoelectric generator); (b) temperature difference between two sides of the TPyP device under different solar intensities, and (c) the corresponding open circuit voltage under the different solar irradiances; (d) cycling performance of the TPyP generator under 1, 2, and 5 sunlight.



enhancement of light intensity, while the temperature difference of the blank thermoelectric sheet is relatively lower. Moreover, this solar power generation device was irradiated with and without 1, 2, and 5 kW m<sup>-2</sup> light for 5 cycles. The experimental results show that the thermoelectric device has excellent durability and cycle stability (Fig. 3d). In addition, under strong light, the electric energy generated by the thermoelectric device coated with TPYP can drive a small fan.

#### 2.4. TPYP for the synergetic coupling of solar-steam and solar-electricity performance

Based on these great results, cellulose + TPYP was integrated with a thermoelectric generator to make an integrated device for simultaneous water evaporation and thermoelectric power generation that truly achieves power generation from waste heat. A polystyrene foam frame was used to fix the thermoelectric generator so that the lower part of the module was immersed in water. Under sunlight, the upper side of the thermoelectric sheet coated with TPYP-cellulose paper attains a higher temperature, while the lower side is cooled by a large amount of water; thereby, the effective temperature difference was generated using low-grade heat to generate electricity while evaporating water. The cellulose paper coated with TPYP was used for water evaporation under sunlight, and the measured water evaporation rate was 0.69 kg m<sup>-2</sup> h<sup>-1</sup> (Fig. 4a). The temperature difference and electrical signal output of the thermoelectric device are recorded in Fig. 4b and e. The maximum  $V_{oc}$  was about 58, 92, and 170 mV, which is caused by the temperature difference of 7.1 °C, 10.2 °C, and 20.4 °C under a solar energy density of 1, 2, and 5 kW m<sup>-2</sup> (Fig. 4c). As the sunlight energy density increases, the temperature difference also increases, resulting in a larger output voltage.

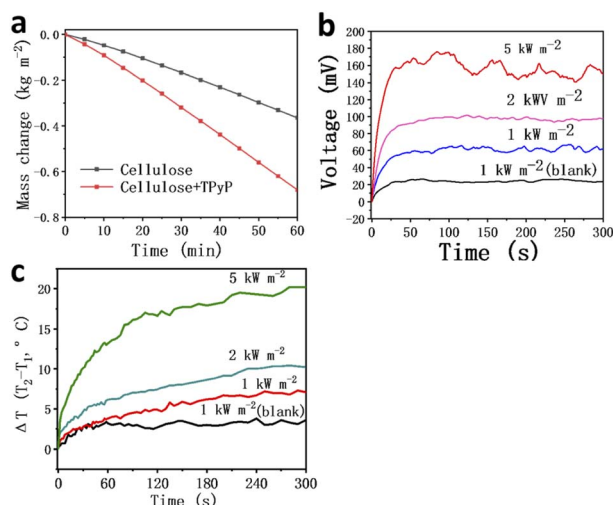


Fig. 4 (a) Evaporative weight loss curve of water-electric cogeneration unit at an optical density of 1 kW m<sup>-2</sup>; (b) corresponding open-circuit voltages under different sunlight densities; (c) temperature difference curves between TPYP cellulose paper surface and water under different sunlight densities.  $\Delta T$  is TPYP cellulose paper surface temperature minus water temperature. Cellulose paper size is 4 × 4 cm<sup>2</sup>, TPYP power dosage is 20 mg.

### 3 Conclusions

In summary, the porphyrin derivative tetrapyrrolylporphyrin (TPYP) was used as the photothermal material, which is a classic polycyclic conjugated compound with polypyrrole macrocyclic framework (18 $\pi$  electrons) and possesses intense molar extinction coefficient, relatively low fluorescence quantum yield, high photostability, and thermal stability. TPYP exhibits wide absorption spectrum of 300–800 nm in solid state, and high thermal/photostability. TPYP shows stable and impressive photothermal properties under 655 nm laser irradiation, and the solid photothermal conversion efficiency was estimated to be 73.6%. Under 1 sunlight irradiation, the solar-to-vapor efficiency and water vapor evaporation rate reached 56% and 0.81 kg m<sup>-2</sup> h<sup>-1</sup> with PU + TPYP foam as the photothermal material for the interfacial-heating evaporation system. In addition, TPYP-loaded cellulose papers equipped with abundant micro-channels for water flow were integrated with thermoelectric devices, thus achieving an evaporation rate and voltage as high as 0.69 kg m<sup>-2</sup> h<sup>-1</sup> and 60 mV under 1 kW m<sup>-2</sup> solar irradiation, respectively. Therefore, the amazing water purification and thermoelectric power generation performance based on the novel organic small-molecular photothermal material TPYP provides a brand new way for energy shortage and bring significant social economic benefits with continuous development.

### Conflicts of interest

There are no conflicts to declare.

### Acknowledgements

This work is grateful for the funding support through Post-doctoral Workstation of State Grid Electric Power Company of Shanxi Province.

### References

- J. J. Urban, *Joule*, 2017, **1**, 665.
- F. R. Fan, W. Tang and Z. L. Wang, *Adv. Mater.*, 2016, **28**, 4283.
- M. J. Montes, A. Abánades and J. M. Martínez-Val, *Sol. Energy*, 2009, **83**, 679.
- C. J. Chen, Y. J. Li, J. W. Song, Z. Yang, Y. Kuang, E. Hitz, C. Jia, A. Gong, F. Jiang, J. Y. Zhu, B. Yang, J. Xie and L. B. Hu, *Adv. Mater.*, 2017, **29**, 8.
- J. Chen, J. Feng, Z. Li, P. Xu, X. Wang, W. Yin, M. Wang, X. Ge and Y. Yin, *Nano Lett.*, 2019, **19**, 400.
- M. M. Gao, L. L. Zhu, C. K. Peh and G. W. Ho, *Energy Environ. Sci.*, 2019, **12**, 841.
- Y. Y. Cui, J. Liu, Z. Q. Li, M. Y. Ji, M. Zhao, M. H. Shen, X. Han, T. Jia, C. L. Li and Y. Wang, *Adv. Funct. Mater.*, 2021, 2106247.
- C. Chang, C. Yang, Y. Liu, P. Tao, C. Song, W. Shang, J. Wu and T. Deng, *ACS Appl. Mater. Interfaces*, 2016, **8**, 23412.



- 9 M. Gao, P. K. N. Connor and G. W. Ho, *Energy Environ. Sci.*, 2016, **9**, 3151.
- 10 M. Zhu, Y. Li, F. Chen, X. Zhu, J. Dai, Y. Li, Z. Yang, X. Yan, J. Song, Y. Wang, E. Hitz, W. Luo, M. Lu, B. Yang and L. Hu, *Adv. Energy Mater.*, 2018, **8**, 1701028.
- 11 X. Huang, W. Zhang, G. Guan, G. Song, R. Zou and J. Hu, *Acc. Chem. Res.*, 2017, **50**, 2529.
- 12 C. Song, T. Li, W. Guo, Y. Gao, C. Yang, Q. Zhang, D. An, W. Huang, M. Yan and C. Guo, *New J. Chem.*, 2018, **42**, 3175.
- 13 Z. Hua, B. Li, L. Li, X. Yin, K. Chen and W. Wang, *J. Phys. Chem. C*, 2017, **121**, 60.
- 14 G. Zhu, J. Xu, W. Zhao and F. Huang, *ACS Appl. Mater. Interfaces*, 2016, **8**, 31716.
- 15 G. Ni, N. Miljkovic, H. Ghasemi, X. Huang, S. V. Boriskina, C.-T. Lin, J. Wang, Y. Xu, M. M. Rahman, T. Zhang and G. Chen, *Nano Energy*, 2015, **17**, 290.
- 16 X. Gao, H. Ren, J. Zhou, R. Du, C. Yin, R. Liu, H. Peng, L. Tong, Z. Liu and J. Zhang, *Chem. Mater.*, 2017, **29**, 5777.
- 17 Y. Wang, L. Zhang and P. Wang, *ACS Sustain. Chem. Eng.*, 2016, **4**, 1223.
- 18 C. Chen, Y. Li, J. Song, Z. Yang, Y. Kuang, E. Hitz, C. Jia, A. Gong, F. Jiang, J. Y. Zhu, B. Yang, J. Xie and L. Hu, *Adv. Mater.*, 2017, **29**, 1701756.
- 19 L. Zhang, B. Tang, J. Wu, R. Li and P. Wang, *Adv. Mater.*, 2015, **27**, 4889.
- 20 X. Huang, Y.-H. Yu, O. de Llergo, S. M. Marquez and Z. Cheng, *RSC Adv.*, 2017, **7**, 9495.
- 21 C.-F. Wang, C.-L. Wu, S.-W. Kuo, W.-S. Hung, K.-J. Lee, H.-C. Tsai, C.-J. Chang and J.-Y. Lai, *Sci. Rep.*, 2020, **10**, 12769.
- 22 M. S. T. Gonçalves, *Chem. Rev.*, 2009, **109**, 190.
- 23 Q. Chen, L. G. Xu, C. Liang, C. Wang, R. Peng and Z. Liu, *Nat. Commun.*, 2016, **7**, 13193.
- 24 S. Zhang, J. Li, J. Wei and M. Yin, *Sci. Bull.*, 2018, **63**, 101.
- 25 Y. Cai, W. Si, Q. Tang, P. Liang, C. Zhang, P. Chen, Q. Zhang, W. Huang and X. Dong, *Nano Res.*, 2017, **10**, 794.
- 26 Y. Liu, N. Song, L. Chen, S. Liu and Z. Xie, *Chem. - Asian J.*, 2018, **13**, 989.
- 27 D. Yao, Y. Wang, R. Zou, K. Bian, P. Liu, S. Shen, W. Yang, B. Zhang and D. Wang, *ACS Appl. Mater. Interfaces*, 2020, **12**, 4276.
- 28 Y. Wang, H. Masunaga, T. Hikima, H. Matsumoto, T. Mori and T. Michinobu, *Macromolecules*, 2015, **48**, 4012.
- 29 H. X. Li, H. F. Wen, J. Li, J. C. Huang, D. Wang and B. Z. Tang, *ACS Appl. Mater. Interfaces*, 2020, **12**, 26033.
- 30 A. Politano, P. Argurio, G. Profio, V. Sanna, A. Cupolillo, S. Chakraborty, H. A. Arafat and E. Curcio, *Adv. Mater.*, 2017, **29**, 1603504.
- 31 G. Y. Chen, J. M. Sun, Q. Peng, Q. Sun, G. Wang, Y. J. Cai, X. G. Gu, Z. G. Shuai and B. Z. Tang, *Adv. Mater.*, 2020, **32**, 1908537.
- 32 X. Han, Z. Y. Wang, M. H. Shen, J. Liu, Y. X. Lei, Z. Q. Li, T. Jia and Y. Wang, *J. Mater. Chem. A*, 2021, **9**, 24452.
- 33 P. Mu, W. Bai, Z. Zhang, J. He, H. Sun, Z. Zhu, W. Liang and A. Li, *J. Mater. Chem. A*, 2018, **6**, 18183.
- 34 X. Wang, Q. Liu, S. Wu, B. Xu and H. Xu, *Adv. Mater.*, 2019, **31**, 1807716.
- 35 S. Wang, S. Li, J. Xiong, Z. Lin, W. Wei and Y. Xu, *Chem. Commun.*, 2020, **56**, 7399.
- 36 N. Rabiee, M. T. Yarak, S. M. Garakani, S. M. Garakani, S. Ahmadi, A. Lajevardi, M. Bagherzadeh, M. Rabiee, L. Tayebi, M. Tahriri and M. R. Hamblin, *Biomaterials*, 2020, **232**, 119707.

